Materials Research Express

ACCEPTED MANUSCRIPT

Electrospinning of gold nanoparticles incorporated PAN nanofibers via in-situ laser ablation of gold in electrospinning solution

To cite this article before publication: Amir Shahin Shamsabadi *et al* 2019 *Mater. Res. Express* in press https://doi.org/10.1088/2053-1591/ab0709

Electrospinning of gold nanoparticles incorporated PAN nanofibers via in-situ laser ablation of gold in electrospinning solution

Amir Shahin Shamsabadi[a], Mehdi Ranjbar[bc], Hossein Tavanai[ac]*, Ameneh Farnood[b]

[a]Department of Textile Engineering, Isfahan University of Technology, Isfahan, 84156-83111 Iran

[b]Department of Physics, Isfahan University of Technology, Isfahan, 84156-83111 Iran

[c]Center of Excellence in Applied Nanotechnology, Nanotechnology and Advanced Materials Institute, Isfahan University of Technology, Isfahan, 84156-83111, Iran.

*Corresponding author: tavanai@cc.iut.ac.ir
Tel: +983133915030, Fax: +983133912444

ABSTRACT

Fabrication of electrospun gold nanoparticle incorporated polyacrylonitrile (PAN) nanofibers via in-situ laser ablation of gold in electrospinning solution is reported. It was found that spherical gold nanoparticles with an average diameter of 17 nm had been synthesized successfully. A monocrystalline morphology was shown for the laser ablated gold nanoparticles in the electrospinning solution and inside the nanocomposite nanofibers. An average diameter in the range of 123 - 317 nm was obtained for the electrospun nanofibers. The gold nanoparticles dispersed in PAN nanofibers showed a face centered cubic crystal structure with an average crystallite size of around 8 nm. A smooth surface was observed for the nanofibers. No gold nanoparticles could be obsreved on the surface of the nanofibers. The gold nanoparticles enjoyed a random distribution inside the nanofibers with no considerable agglomeration. No reaction or interaction could be observed between PAN and the gold nanoparticles.

Key Words: Laser ablation; gold nanoparticles; electrospun PAN nanofibers

1. Introduction

Transition metal nanoparticles have attracted a lot of interest because of their specific properties [1-3] and application in electrical [4], optical [5], magnetic [6], catalytic, chemical and biochemical sensing technologies [7]. Among transition metal nanoparticles, the noble ones (especially gold and silver) have been extensively studied for sensor applications [8], thanks to their unique optical properties including tunable surface plasmon resonances [9], surface-enhanced Raman scattering (SERS) [10] and highly enhanced fluorescence intensity [11]. However, when compared with silver, characteristics like shape and size dependent optical properties known as localized surface plasmon resonance (LSPR), non-linear optical properties (NLO) and quantized charging effects are more pronounced for gold [11-13]. Gold nanoparticles are finding use in a range of applications especially nanobiosensor, biomedicine, and nanophotonics [14, 15]. It must be pointed out that nano sized materials enjoy much greater specific surface areas and in the case of noble metals (Au, Ag, and Cu) higher degree of quantum confinement effect [16, 17].

In general, two approaches namely chemical and physical are employed for the synthesis of gold nanoparticles. The chemical approach which includes mainly, citrate reduction, the Brust-Schiffrin method, and electroless deposition requires various auxiliary materials and is rather difficult to carry out. In contrast, the physical approaches like radiolysis, thermolysis and laser ablation are simpler and do not require any harmful auxiliaries. Among the physical approaches, laser ablation is more common because apart from producing stable dispersions for a long time, it is relatively fast and can be carried out at ambient temperature. Moreover, it yields higher purity (thanks to the direct incidence of laser beam on the target) and can be carried out on a number of targets in different solvents. [18, 19].

Laser ablation synthesis in solution (LASiS) is an efficient physical method for the synthesis of noble-metal nanoparticles. To carry out laser ablation, the target is irradiated by a pulsed laser beam. The excitation of the electrons of the target by laser beam causes a temperature rise of the target surface, to an extent that atoms leave the target and form a bubble above the target surface. In the next stage, the atoms aggregate to form nanoparticles as they leave the bubble and propagate in the media e.g. a polymeric solution (PAN in the case of the present work). In fact, the final solution can be considered as a dispersion of the newly synthetized nanoparticles [12, 20, 21]. Laser ablation method has been introduced by Henglein, Cotton and their coworkers in early 1990s [22, 23]. However Mafuné et al. developed this method further for producing gold nanoparticles [24]. A schematic representation of nanoparticle synthesis through laser ablation has been shown in Figure 1. LASiS can be carried out with two targets in solution at the same time which leads to a final dispersion of the so called multi-particles or alloy nanoparticles. The conditions of the solution can affect the size and the shape of the ablated particles [20, 25].

Employment of nanoparticles for different applications, requires embedding and immobilization in a matrix like polymers. Nanoparticles and nanofilms are examples of zero and two dimensional nano structures, respectively. However, nanowires, nanorods, nanotubes and nanofibers constitute the one dimensional matrices [14, 26, 27]. As far as electrical conductivity is concerned, nanofibers can provide faster electron transport because, nanoparticles can arrange themselves in one direction much easier than other nanostructures [1]. The high aspect ratio as well as high flexibility and versatility of fibers considered as their merits [4]. Electrospinning has proved to be a simple, versatile and cost-effective approach for produce polymeric nanofibers[28].

The literature review on the electrospun nanofibers either incorporated or coated with gold nanoparticles (dating back only to 2005) is summarized as follows.

Kim et al. [29] were the first to report the electrospinning of poly (ethylene oxide) nanofibers incorporated with gold nanoparticles. In this work, a dispersion of ready to use gold nanoparticles in poly (ethylene oxide) solution was electrospun. In 2006, Wang et al. [27] electrospun PVP nanofibers incorporated with gold nanoparticles (average diameter = 20 nm). These nanoparticles were synthesized in an aqueous solution in which $HAuCl_4$ was reduced by trisodium citrate. To prepare the electrospinning solution, the synthesized gold nanoparticles were added to the PVP solution in ethanol. No information on the application of these two products has been given in the corresponding references.

The works employing in-situ chemical synthesis of gold nanoparticles on the surface of nanofibers are summarized as follows:

In 2006, Han et al. [30] coated a gold salt incorporated electrospun poly(methyl methacrylate) fibrous mats with a layer of conductive gold film through a self-catalyzed reduction mechanism, using $NaBH_4$ as reducing agent. The average size of the gold nanoparticles deposited on the surface of nanofibers has been reported to be up to 100 nm. Also in 2006, Dong et al. [2] synthesized gold nanoparticles on electrospun poly(4-vinylpyridine) nanofibers by dipping the nanofibers in a $NaCl_4$ solution with subsequent reduction by $NaBH_4$. No information has been made available on the application of these nanofibers as well. In 2010 Marx et al. [31] reported the electrospinning of a PAN solution containing $HAuCl_4$. The electrospun fibers were first reduced by immersion in $NaBH_4$ solution, and then gold nanoparticles (93 nm) was deposited through electroless technique, by dipping the fibers into an aqueous solution containing hydroxylamine hydrochloride and $HAuCl_4$. This product was used

as an electrode in biosensors for detecting glucose and fructose. In 2011 Fang et al. [32] synthesized gold nanoparticles on the surface of cross-linked polyethyleneimine/polyvinyl alcohol hybrid nanofibers through reaction with $HAuCl_4$. As a result, immobilization of Au nanoparticles occurred when free amine groups of polyethyleneimine reacted with $AuCl^{4-}$. Applications of this product include catalysis, sensing, and biomedical sciences. In 2015, Liu et al. [14] electrospun 4-(dimethylamino) benzaldehyde (reductant) incorporated PAN nanofibers and then synthesized gold nanoparticles (6 nm) on the fiber surface by chemical reduction of Au(III). They demonstrated that this product showed great potential in the field of electrocatalysis and chemo/biosensors.

The works employing in-situ chemical synthesis of gold nanoparticles in electrospinning solution are as follows:

In 2007, Baie et al. [11] electrospun poly (vinyl alcohol) nanofibers containing gold nanoparticles with size in the range of 10 - 11 nm. They used trisodium citrate to reduce $HAuCl_4$ in poly (vinyl alcohol) solution which led to the formation of gold nanoparticles. Again, the application of this product has not been disclosed. In 2015, Serbezeanu et al. [33] electrospun the mixture of $HAuCl_4$ and Polyimide in DMF solution. In order to reduce Au^{3+} ($HAuCl_4$) to Au^0 (size in the range of 8-20 nm), the nanofibers were treated at 200°C. It is claimed that these nanofibers (with tunable optical properties) can find applications as catalysts.

Considering the above mentioned literature review, in the present work, it was decided to laser ablate gold in polyacrylonitrile (PAN) solution in DMF, with the aim of obtaining a stable dispersion of gold nanoparticles directly, suitable for electrospinning with no need to add any dispersing agent or using sonication. It is reminded that the dispersions of this kind keep their stability for months. The gold nanoparticles incorporated electrospun PAN nanofibers were

characterized in the second stage of the work. It must be pointed out that in–situ laser ablation of gold (a physical approach) in electrospinning solution, constitutes the novelty of the present work.

2. Experimental

2.1 Materials

PAN powder ($\bar{M}_n$ = 7 × 10^5 g/mol, $\bar{M}_w$ = 106 g/mol), acrylonitrile (94 wt %), methyl methacrylate (4 wt %), and methacrylic acid (2 wt %) was provided by Iran Polyacryl Company. DMF was purchased from Merck, Germany. The gold plate used as the target of the laser ablation had a purity of 99.99%. All materials were used as received.

2.2 Preparation of PAN solutions

PAN solutions were prepared by adding 6, 7, 8 and 9 w/v % PAN powder to DMF and stirred for 12h at room temperature to ensure complete dissolution. 5, 10 and 50 ml of the prepared solutions were chosen for the laser ablation of gold.

2.3 Synthesis of gold nanoparticles by laser ablation of gold in PAN solution

A beam of a Cd:Nd:YAG laser (Shafaparto QPm60, Iran, λ = 1064 nm, τ = 5 ns, R.R = 10 Hz, 600 mJ energy per pulse) was employed for the laser ablation of the gold target. The spot size of the focused beam at the target surface was 1 mm^2. The ablation time for all the samples was 30 min. In order to obtain three different concentrations of gold nanoparticle in the final electrospinning solutions, three different volumes namely, 5, 10 and 50 ml of PAN solutions with different PAN concentrations (6, 7, 8 and 9 w/v %) were chosen for ablation. In this way, a total of 12 electrospinning solutions were prepared.

2.4 Determination of gold nanoparticle concentration in electrospinning solutions

The concentration of gold nanoparticles in the 12 electrospinning solutions was determined by using inductively coupled plasma optical emission spectroscopy (ICP-OES) (Perkin Elmer Optima 7300 DV, USA). The required optical properties namely, maximum wavelength and maximum absorption for concentration measurements were determined by Lambda 25 spectrophotometer (Perkin Elmer, USA). The range of the wavelength was 200–1100 nm.

2.5 Measurement of electrical conductivity, viscosity and surface tension of electrospinning solutions

The electrical conductivity, viscosity and surface tension of electrospinning solutions were measured by electrical conductivity meter (Hoorteb SANA SL-901, Iran), viscometer (Brookfield DV-II, USA) and surface tension measuring device (Dataphysics 11DCAT, Germany), respectively.

2.6 Characterization of the morphology of gold nanoparticles in electrospinning solutions

The morphology of the nanoparticles was observed by transmission electron microscopy (TEM, Philips CN30 150 and 200 kV, Netherlands) and Dynamic light scattering (DLS) (Orduan Technologies VASCO Flex TM, France).

2.7 Electrospinning

The electrospinning set up consisted of a high voltage supply (up to 30 kV DC output), a pump (MS-2200 DAIWHA, South Korea) with feeding capacity of 0–60 ml/h, and a 1 ml syringe with a blunt tipped needle (internal diameter = 0.5 mm). The blunt needle tip was connected to the positive electrode and the aluminum foil collector was connected to negative electrode. The electrospun PAN nanofibrous web incorporated with gold nanoparticles was collected on aluminum foil.

2.8 Characterization of the electrospun nanofibers

Scanning electron microscope (SEM, Philips XL 30, Holland and Zeis, DSM-162A, Germany) and field emission scanning electron microscope (FESEM, Tescan MIRA2TESCAN-XMU, Czech Republic) were used to study the morphology of the electrospun nanofibers. The SEM micrographs were used for the measurement of the average diameter of nanofibers (replica = 100) with the help of Digimizer 4.3.5 software (MedCalc Software, Belgium). The distribution of gold nanoparticles inside the nanofibers were observed by transmission electron microscopy (TEM, Philips CN30 150 and 200 kV, Netherlands). To analyze any reaction or interaction between PAN and gold nanoparticles, FTIR (BOMEM–MB Series, Hartmann & Braun, Canada) was employed. To carry out micro structural analysis, XRD (Asenware AW-XDM300, UK) was used.

3. Results and discussion

3.1 Characterization of the electrospinning solutions

In order to characterize the electrospinning solutions, the size, shape and concentration of gold nanoparticles in the solutions as well as the viscosity, surface tension and electrical conductivity of the solutions were measured.

Figure 2 shows the optical absorption spectra of the 5 ml (a), 10 ml (b) and 50 ml (c) of the dispersion of gold nanoparticles in PAN solution (8% w/v). As can be seen, all the three samples show an absorption plasmonic peak at 526 nm. The wavelength of the plasmonic peak depends on the material, concentration, size and shape of nanoparticles [34]. So, it is concluded that the plasmonic peak at 526 nm proves the existence of gold nanoparticles. Moreover, the shape of the curves implies a similar average size and shape of the gold nanoparticles in all the

three solutions. The only difference is due to the concentration of gold nanoparticles which is shown by the height of the peaks. According to the calculations using the intensity of the peaks and the data provided by ICP, the concentration of gold nanoparticles in the solutions a, b, and c were calculated to be 295.8, 165.5 and 108.2 mg/l. Expressing these concentrations in terms of percentage gives about 0.03, 0.02% and 0.01 % (w/v) for samples a, b, and c, respectively.

Figure 3 shows the TEM image and the corresponding SAED pattern of the electrospinning solution with gold nanoparticle concentration of 0.02% w/v (PAN solution 8% w/v). As it can be seen, the gold nanoparticles have a spherical shape with an average size of 17 nm (Figure 4a). As already explained, Digimizer software was employed to calculate the average size of the nanoparticles. It must be pointed out that generally the depth of the shade (contrast) of the TEM image of nanoparticles depends on the atomic number of the elements as well as their packing density. A higher depth shows a higher atomic number as well as a higher packing density. Moreover, the SAED pattern shows a monocrystalline structure for the gold nanoparticles in the solution. Basically, monocrystalline structures are formed from an orderly arrangement of crystallite network, whereas a randomly arranged order of crystallites is defined as polycrystalline structure [35, 36].

Figure 4b shows the DLS spectra of the electrospinning solution with gold nanoparticle concentration of 0.02% w/v (PAN solution 8% w/v). An average diameter of 47 nm is reported for the nanoparticles. Compared to the TEM image, the higher average particle size by DLS is related to the much higher number of particles considered for measurement, which can be considered as a more meaningful value. Moreover, the bigger nanoparticle size could be related to the halo formed around the nanoparticles during DLS analysis.

Table 1 shows the average diameter (replica = 100) of the electrospun nanofibers versus the concentration of PAN and gold nanoparticles, viscosity, electrical conductivity and surface tension of the corresponding electrospinning solutions.

As expected, increasing the concentration of PAN as well as gold nanoparticles increases the viscosity of the solutions. However, as far as the surface tension of the solutions is concerned, in spite of a very small decreasing trend in surface tension with increasing amount of PAN and gold nanoparticles, the differences are practically insignificant. Table 1 also shows that in spite of a decreasing trend with a slow slope, the effect of increasing PAN concentration on the electrical conductivity of the solutions is negligible. However, the impact of increasing gold nanoparticle concentration on the electrical conductivity of the solutions is considerable (increasing trend). These data will be used later to explain the dependence of the average diameter of the electrospun gold nanoparticle incorporated PAN nanofibers on the three above mentioned electrospinning material variables.

3.2 Morphological analysis of the electrospun nanofibers

Figure 5 shows a typical SEM image of the electrospun Au (0.01% w/v)/PAN (6 and 7% w/v) fibers under different electrospinning conditions. As can be seen, in spite of trying different conditions of electrospinning, with PAN concentrations of 6 and 7% in the electrospinning solutions, no proper nanofibers could be electrospun. Figure 6 shows the SEM images of Au (0.01% w/v)/PAN (8% and 9% w/v) nanofibers. The electrospinning conditions were; voltage = 11 kV, nozzle–collector distance =15 cm and feed rate=0.075 ml/h. These optimum electrospinning conditions were also applied to the rest of the electrospinning trials carried out in this work. However, as can be seen, from the two concentrations of 8 and 9%, only the 8% one yielded proper electrospun nanofibers with an average diameter of 317 nm. To obtain lower

diameters, the electrical conductivity of the electrospinning solutions was increased by increasing the concentration of gold nanoparticles to 0.02% in the electrospinning solutions with PAN concentrations of 6, 7, 8 and 9%. The SEM images of the resulting electrospun nanofibers are shown in Figure 7(a, b, c, and d). As can be seen electrospinning of PAN solutions (8% and 9%) containing 0.02% gold nanoparticles led to the formation of rather uniform nanofibers with an average diameter of 123 nm and 176 nm, respectively. It is worth mentioning that the diameter of 8% sample showed a lower standard deviation. The 8% sample showed less beads as well.

In a further effort to make the solutions containing 6% and 7% PAN electrospinnable, the amount of gold nanoparticle was raised to 0.03%. Figure 8 shows the SEM images of the electrospun nanofibers with an average nanofiber diameter of 140 nm and 244 nm for PAN concentrations of 6% and 7%, respectively. As can be seen, raising the gold nanoparticle concentration to 0.03% made the electrospinning of uniform and almost bead-free nanofibers from only 7% PAN concentration possible.

Considering the insignificant difference between the surface tension of the electrospinning solutions it is concluded that:

- With constant gold nanoparticle concentrations of 0.02% and 0.03% w/v, increasing PAN concentration, leads to higher average diameter of nanofibers as expected [37]. This is related to higher viscosity as a result of higher PAN concentration. Higher viscosities raise the resistance against the electric field which tries to draw the electrospun nanofibers [38]

- With constant PAN concentration (8% w/v), increasing gold concentration leads to lower average diameter for the electrospun nanofibers as expected [39]. This decrease is related to the

higher electrical conductivity of the electrospinning solution with larger amount of gold nanoparticles which enjoy high electrical conductivity. In fact, higher conductivity leads to lower average nanofiber diameter as expected. Higher electrical conductivity eases the drawing of the air-born nano filaments in the electrospinning field [40].

-Available reports on the electrospinning of PAN solutions containing metals (Ag, Cu, etc.) or metal oxide (MgO, Al_2O_3, SiO_2, etc.) nanoparticles reveal that a minimum PAN concentration of 12% has been required to electrospin uniform nanofibers [28, 41-43], whereas, as observed in this work, incorporating gold nanoparticles makes the electrospinning of PAN solutions with PAN concentration as low as 6% possible.

- High average diameter of 244 nm, in spite of high electrical conductivity of the corresponding electrospinning solution shows the dominance of viscosity over electrical conductivity for the above mentioned cases.

-High average diameter of the 317 nm, in spite of the low viscosity of the corresponding electrospinning solution, shows the dominance of low conductivity over viscosity.

3.3 Characterization of the electrospun nanofibers

To characterize the electrospun nanofibers, the PAN/Au sample from the dispersion of gold nanoparticles (0.02% w/v) in 8% w/v PAN solution (electrospinning conditions: voltage = 11 kV, nozzle – collector distance =15 cm and feed rate = 0.075 ml/h) was chosen to represent all the 5 electrospun nanofibers. This sample was the most uniform and enjoyed the lowest average fiber diameter.

The corresponding XRD analysis is shown in Figure 9, depicting the patterns of pure PAN as well as gold nanoparticle incorporated PAN nanofibers. As can be seen, the XRD

patterns show gold nanoparticle crystals with characteristic peaks at 2Θ = 38, 44, 65, 78 degrees dispersed in a rather semi crystalline PAN matrix. According to JCPDS card No. 00-002-1095, these characteristic peaks show a face centered cubic (fcc) crystal structure for the gold nanoparticles dispersed in PAN matrix. Using Scherrer equation [44] gives an average crystallite size of around 8 nm. For further analysis on gold nanoparticle crystals, the SAED pattern in Figure. 16 will be considered later.

In order to investigate the distribution of gold nanoparticles on the surface and inside of the electrospun nanofibers, FESEM as well as TEM analysis were carried out. Figures 10 and 11 show the corresponding FESEM and TEM images. The FESEM image shows an even surface for the nanofibers with no sign of gold nanoparticles on it, implying that the gold nanoparticles are tactfully held inside the nanofibers. This is proved by the TEM images which show a random distribution of the gold nanoparticles inside the fibers. This is a sign of a homogenous dispersion of gold nanoparticles in the PAN solutions. As already stated in the introduction part, producing stable dispersions is a merit of laser ablation. Measuring the size of nanoparticles (n = 60) from the TEM images shows an average diameter of around 19 nm with minimum and maximum size of 8 nm and 34 nm, respectively. Comparing the obtained statistics with those obtained from the TEM image of the corresponding electrospinning solution (Average = around 17 nm, Min = 7.5 nm, Max = 34nm) shows that gold nanoparticles have not gone through any considerable agglomeration during electrospinning.

Figure 11 also shows the corresponding SAED pattern of the electrospun nanofibers. As can be seen, the pattern is very similar to that of gold nanoparticles in PAN solution (Figure 3) with a darker background which is related to the solidification of PAN molecules in the nanofibers. However, as far as the morphology is concerned, it is concluded that the gold

Nnanoparticles inside the nanofibers have kept their original monocrystalline structure in the electrospinning solution. As already explained monocrystalline structures are formed from an orderly arrangement of crystallite network.

The FTIR spectras of electrospun pure PAN and PAN/Au nanofibers are shown in Figure 12. As can be seen, the spectrum of gold nanoparticle incorporated PAN nanofibers shows all the characteristic peaks of PAN [45, 46] with no additional ones. It is concluded that as expected, considering the very high unreactivity of gold, no reaction or interaction has occurred between PAN and the gold nanoparticles. The higher intensity of peaks at wavelengths of 1666 nm and 2245 nm for PAN/Au nanofibers may be a result of higher absorption of infrared due to lower electrostatic interaction between C≡N groups of PAN which in turn can be related to the presence of monocrystalline gold nanoparticles within the polymeric chains.

4. Conclusions

Gold nanoparticles with average diameter of 17 nm were synthesized successfully in-situ, by laser ablation in the solution of PAN in dimethyl formamide. Absorbtion plasmonic peak at 526 nm proved the existence of spherical gold nanoparticles. The SAED pattern indicated a monocrystalline morphology for the laser ablated gold nanoparticles in the electrospinning solution and in the electrospun nanofibers. Gold nanoparticle incorporated nanofibers with an average diameter in the range of 123 - 317 nm were successfully electrospun. The XRD analysis proved that the average crystallite size of gold nanoparticles was around 8 nm. The crystallites show a face centered cubic unit cell. FESEM images demonstrated a smooth surface for the nanofibers with no sign of any gold nanoparticles laying on the surface of the nanofibers. The absence of gold nonoparticles on the surface of nanofibers was further confirmed by TEM images which also showed a clear and random distribution of the gold nanoparticles inside the

PAN naofiberous matrix. Comparison of the average size of nanoparticle in the electrospinning solution with those in nanofibers showed that no considerable agglomeration has occurred during electrospinning. Absence of any reaction or interaction between PAN and the gold nanoparticles was revealed by FTIR analysis. Further work on the application of these nanofibers as a precursor for the fabrication of glucose sensors has been carried out which will be reported in another communication.

Acknowledgement

The authors are grateful to Dr. Farzaneh Alihosseini and Prof. Mohammad H. Enayati for the generous consultations. The authors also would like to thank Mrs. Jinoos Javadi for her collaboration in this work.

5. References

[1] Mondal K, Ali M A, Agrawal V V, Malhotra B D and Sharma A 2014 Highly sensitive biofunctionalized mesoporous electrospun TiO2 nanofiber based interface for biosensing *ACS Appl. Mater. Interfaces* 6 2516-27

[2] Dong H, Fey E, Gandelman A and Jones W E 2006 Synthesis and assembly of metal nanoparticles on electrospun poly (4-vinylpyridine) fibers and poly (4-vinylpyridine) composite fibers *Chem. Mater* 18 2008-11

[3] Liu D, Zhang C, Dong G, Xu C, Liu D, Lv Y, Zhong B and Wang B 2018 Temperature-controlled electrospinning of EVOH nanofibre mats encapsulated with Ag, CuO, and ZnO particles for skin wound dressing *Mater Res Express* 6 015007

[4] Wu H, Hu L, Rowell M W, Kong D, Cha J J, McDonough J R, Zhu J, Yang Y, McGehee M D and Cui Y 2010 Electrospun metal nanofiber webs as high-performance transparent electrode *Nano Lett* 10 4242-8

[5] Wang P, Zhang L, Xia Y, Tong L, Xu X and Ying Y 2012 Polymer nanofibers embedded with aligned gold nanorods: a new platform for plasmonic studies and optical sensing *Nano Lett* 12 3145-50

[6] Wu H, Zhang R, Liu X, Lin D and Pan W 2007 Electrospinning of Fe, Co, and Ni nanofibers: synthesis, assembly, and magnetic properties *Chem. Mater* 19 3506-11

[7] Wang W, Zhang L, Tong S, Li X and Song W 2009 Three-dimensional network films of electrospun copper oxide nanofibers for glucose determination *Biosens. Bioelectron* 25 708-14

[8] Lee H O, Kim E M, Yu H, Jung J-S and Chae W S 2009 Advanced porous gold nanofibers for highly efficient and stable molecular sensing platforms *Nanotechnology* 20 325604

[9] Usman A I and Aziz A A 2018 Optimization of biosynthesis gold nanoparticles via central composite design toward monodisperse *Mater Res Express* 6 015051

[10] Stiles P L, Dieringer J A, Shah N C and Van Duyne R P 2008 Surface-enhanced Raman spectroscopy *Annu. Rev. Anal. Chem.* 1 601-26

[11] Bai J, Li Y, Yang S, Du J, Wang S, Zheng J, Wang Y, Yang Q, Chen X and Jing X 2007 A simple and effective route for the preparation of poly (vinylalcohol)(PVA) nanofibers containing gold nanoparticles by electrospinning method *Solid State Commun* 141 292-5

[12] Nouraddini M, Ranjbar M, Dobson P, Farrokhpour H, Johnston C and Jurkschat K 2017 Stabilized gold nanoparticles by laser ablation in ferric chloride solutions *Appl. Phys. A* 123 727

[13] Chang W, Liu S, Qileng A, Liu W and Liu Y 2018 In-situ synthesis of monodispersed Au nanoparticles on eggshell membrane by the extract of Lagerstroemia speciosa leaves for the catalytic reduction of 4-nitrophenol *Mater Res Express* 6 015002

[14] Liu Z, Zhou C, Zheng B, Qian L, Mo Y, Luo F, Shi Y, Choi M M and Xiao D 2011 In situ synthesis of gold nanoparticles on porous polyacrylonitrile nanofibers for sensing applications *Analyst* 136 4545-51

[15] David T M, Wilson P, Ramesh C, Murugesan N and Sagayaraj P 2018 Influence of noble metal loading and effect of temperature on the hydrogen sensing behavior of the platinum sensitized titania nanotubes *Mater Res Express* 6 015006

[16] El-Sayed M A 2001 Some interesting properties of metals confined in time and nanometer space of different shapes *Acc. Chem. Res* 34 257-64

[17] Zhi M, Xiang C, Li J, Li M and Wu N 2013 Nanostructured carbon–metal oxide composite electrodes for supercapacitors: a review *Nanoscale* 5 72-88

[18] Cao G 2004 *Nanostructures & nanomaterials: synthesis, properties & applications*: Imperial college press)

[19] Sheykhifard Z, Ranjbar M, Farrokhpour H and Salamati H 2015 Direct fabrication of Au/Pd (II) colloidal core-shell nanoparticles by pulsed laser ablation of gold in PdCl2 solution *J. Phys. Chem. C* 119 9534-42

[20] Amendola V and Meneghetti M 2013 What controls the composition and the structure of nanomaterials generated by laser ablation in liquid solution *Phys. Chem. Chem. Phys* 15 3027-46

[21] Amendola V, Polizzi S and Meneghetti M 2006 Laser ablation synthesis of gold nanoparticles in organic solvents *J. Phys. Chem. B* 110 7232-7

[22] Fojtik A and Henglein A 1993 Laser ablation of films and suspended particles in a solvent: formation of cluster and colloid solutions *Ber. Bunsenges. Phy. Chemie* 97 252-4

[23] Sibbald M S, Chumanov G and Cotton T M 1996 Reduction of cytochrome c by halide-modified, laser-ablated silver colloids *J. Phys. Chem* 100 4672-8

[24] Mafuné F, Kohno J, Takeda Y, Kondow T and Sawabe H 2001 Formation of gold nanoparticles by laser ablation in aqueous solution of surfactant *J. Phys. Chem. B* 105 5114-20

[25] Amendola V, Scaramuzza S, Carraro F and Cattaruzza E 2017 Formation of alloy nanoparticles by laser ablation of Au/Fe multilayer films in liquid environment *J. Colloid Interface Sci* 489 18-27

[26] Ömür B C 2018 Humidity effect on adsorption kinetics of ammonia onto electrospun SnO 2 nanofibers *Mater Res Express*

[27] Wang Y, Li Y, Sun G, Zhang G, Liu H, Du J, Yang S, Bai J and Yang Q 2007 Fabrication of Au/PVP nanofiber composites by electrospinning *J. Appl. Polym. Sci* 105 3618-22

[28] Dadvar S, Tavanai H and Morshed M 2014 Fabrication of nanocomposite PAN nanofibers containing MgO and Al 2 O 3 nanoparticles *J. Polym. Sci. A* 56 358-65

[29] Kim G-M, Wutzler A, Radusch H-J, Michler G H, Simon P, Sperling R A and Parak W J 2005 One-dimensional arrangement of gold nanoparticles by electrospinning *Chem. Mater* 17 4949-57

[30] Han G, Guo B, Zhang L and Yang B 2006 Conductive gold films assembled on electrospun poly (methyl methacrylate) fibrous mats *Adv. Mater* 18 1709-12

[31] Marx S, Jose M V, Andersen J D and Russell A J 2011 Electrospun gold nanofiber electrodes for biosensors *Biosens. Bioelectron* 26 2981-6

[32] Fang X, Ma H, Xiao S, Shen M, Guo R, Cao X and Shi X 2011 Facile immobilization of gold nanoparticles into electrospun polyethyleneimine/polyvinyl alcohol nanofibers for catalytic applications *J. Mater. Chem* 21 4493-501

[33] Serbezeanu D, Popa A M, Sava I, Carja I-D, Amberg M, Rossi R M and Fortunato G 2015 Design and synthesis of polyimide–gold nanofibers with tunable optical properties *Eur. Polym. J* 64 10-20

[34] Amendola V and Meneghetti M 2009 Laser ablation synthesis in solution and size manipulation of noble metal nanoparticles *Phys. Chem. Chem. Phys* 11 3805-21

[35] Fuku X, Matinise N, Masikini M, Kasinathan K and Maaza M 2018 An electrochemically active green synthesized polycrystalline NiO/MgO catalyst: use in photo-catalytic applications *Mater. Res. Bull* 97 457-65

[36] Cao Z, Li H, Zhan C, Zhang J, Wang W, Xu B, Lu F, Jiang Y, Xie Z and Zheng L 2018 Monocrystalline platinum–nickel branched nanocages with enhanced catalytic performance towards the hydrogen evolution reaction *Nanoscale* 10 5072-7

[37] He J H, Wan Y Q and Yu J Y 2008 Effect of concentration on electrospun polyacrylonitrile (PAN) nanofibers *Fiber. Polym., J* 9 140-2

[38] Drew C, Wang X, Samuelson L A and Kumar J 2003 The effect of viscosity and filler on electrospun fiber morphology *J Macromol Sci B* 40 1415-22

[39] Heikkilä P and Harlin A 2009 Electrospinning of polyacrylonitrile (PAN) solution: Effect of conductive additive and filler on the process *Express Polym Lett* 3 437-45

[40] Sawicka K M and Gouma P 2006 Electrospun composite nanofibers for functional applications *J. Nanoparticle Res* 8 769-81

[41] Wang T and Kumar S 2006 Electrospinning of polyacrylonitrile nanofibers *J. Appl. Polym. Sci* 102 1023-9

[42] Yang Q, Li D, Hong Y, Li Z, Wang C, Qiu S and Wei Y 2003 Preparation and characterization of a PAN nanofibre containing Ag nanoparticles via electrospinning. In: *ICSM 2002: Proceedings of the 2002 International Conference on Science and Technology of Synthetic Metals*: Elsevier SA) pp 973-4

[43] Ji L, Saquing C, Khan S A and Zhang X 2008 Preparation and characterization of silica nanoparticulate–polyacrylonitrile composite and porous nanofibers *Nanotechnology* 19 085605

[44] Burton A W, Ong K, Rea T and Chan I Y 2009 On the estimation of average crystallite size of zeolites from the Scherrer equation: a critical evaluation of its application to zeolites with one-dimensional pore systems *Micropor. Mesopor. Mat* 117 75-90

[45] Arshad S N, Naraghi M and Chasiotis I 2011 Strong carbon nanofibers from electrospun polyacrylonitrile *Carbon* 49 1710-9

[46] Neghlani P K, Rafizadeh M and Taromi F A 2011 Preparation of aminated-polyacrylonitrile nanofiber membranes for the adsorption of metal ions: Comparison with microfibers *J. Hazard. Mater* 186 182-9

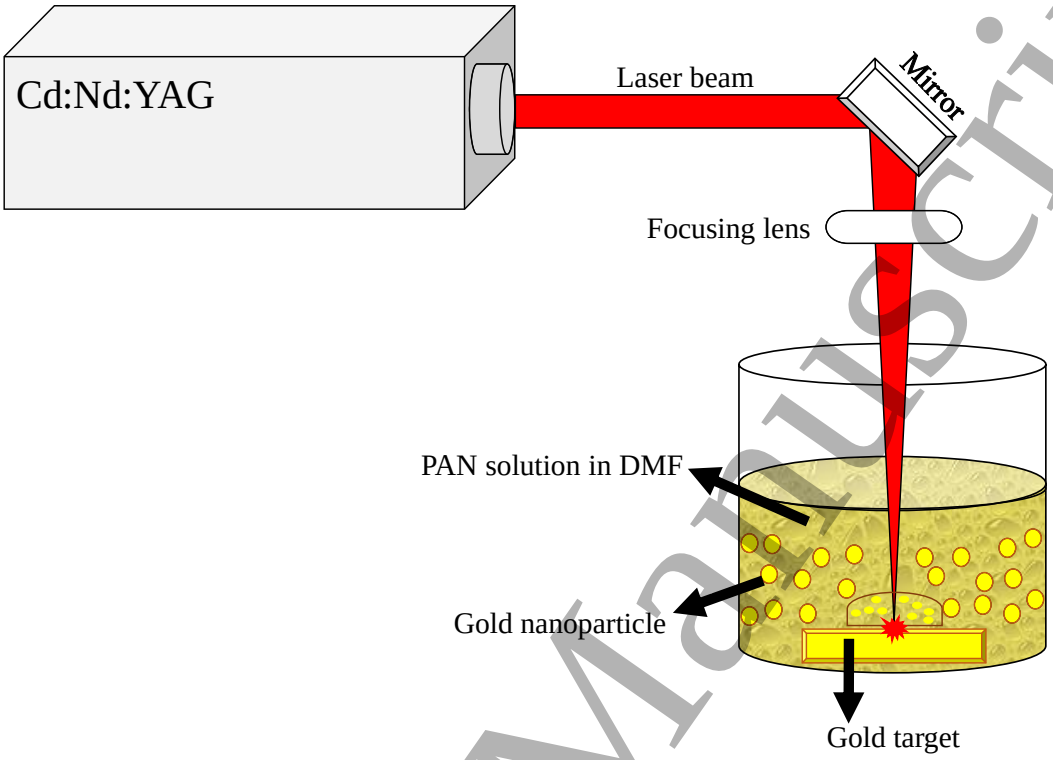

Figure 1. Schematic representation of nanoparticle synthesis through laser ablation

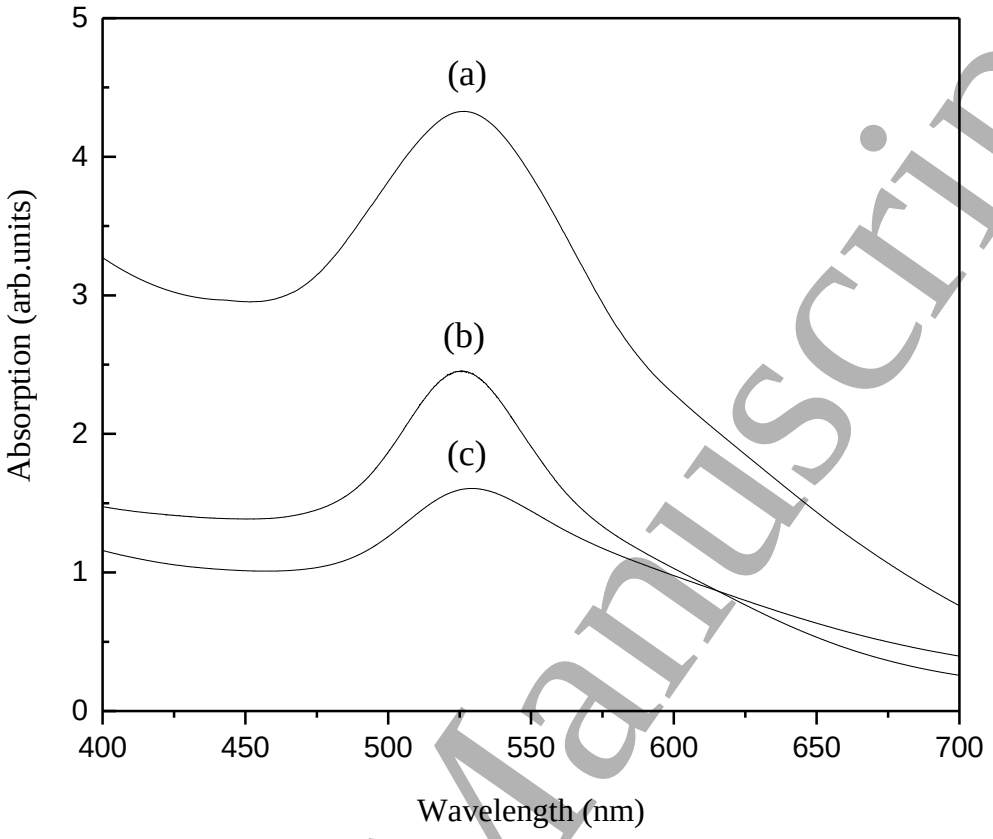

Figure 2. Optical absorption spectra of three volumes of the dispersion of gold nanoparticles in PAN solution (8% w/v), (a) 5 ml; (b) 10 ml; (c) 50 ml

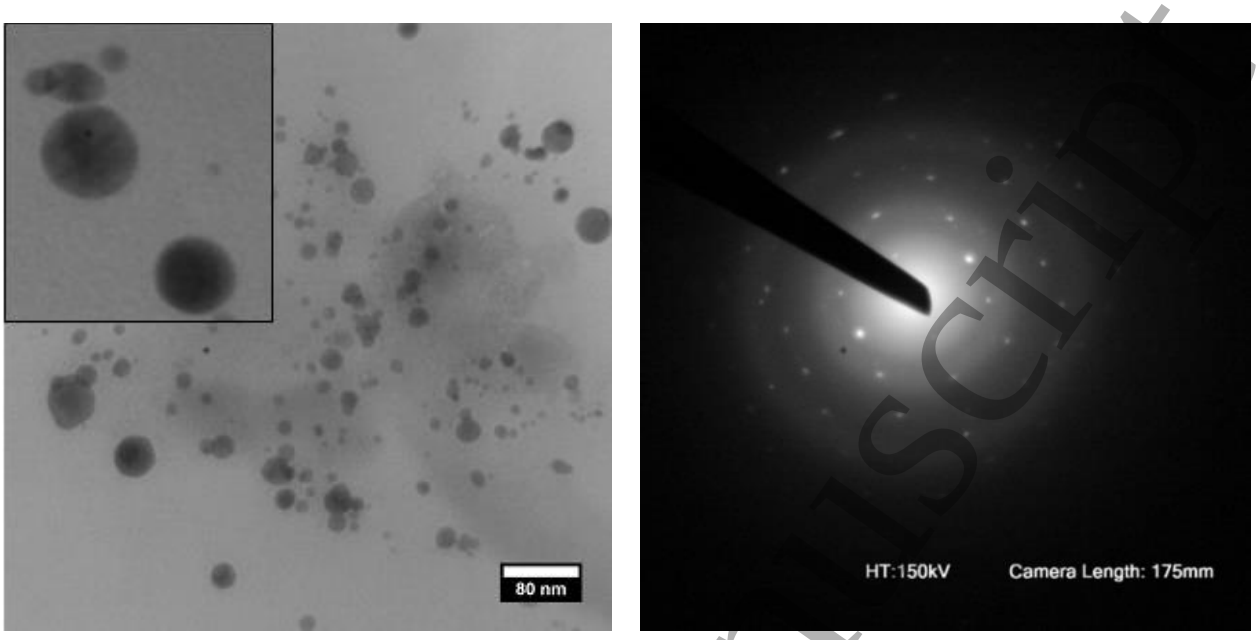

Figure 3. TEM image, nanoparticle size distribution and the corresponding SAED pattern of the laser ablated gold nanoparticles (0.02 % w/v) in PAN solution (8% w/v)

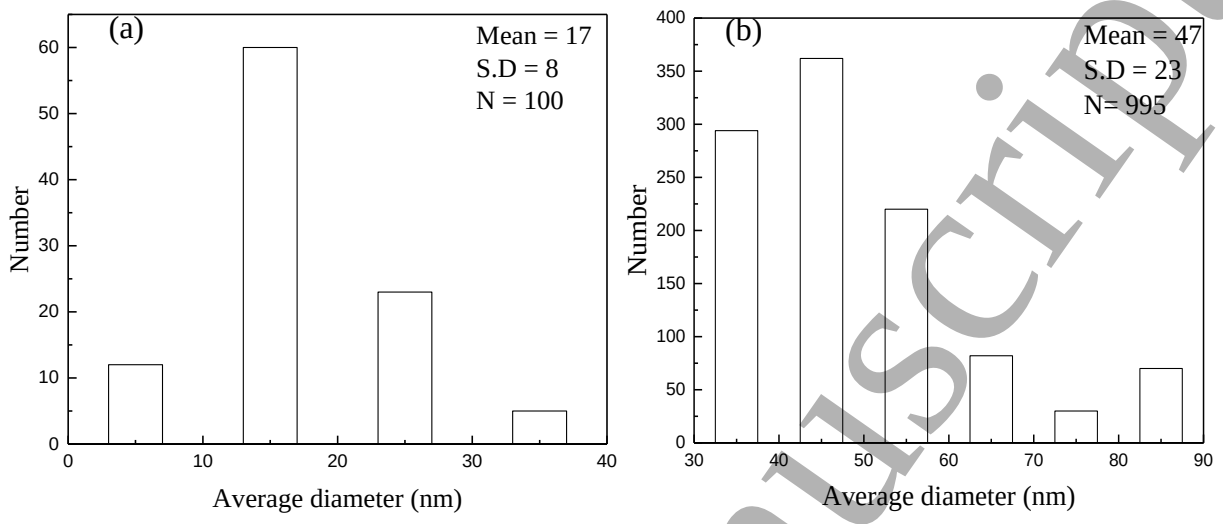

Figure 4. Particle size distribution of gold nanoparticles in the electrospinning solution with gold nanoparticle concentration of 0.02 % w/v (PAN solution 8% w/v) (a) TEM images, (b) DLS

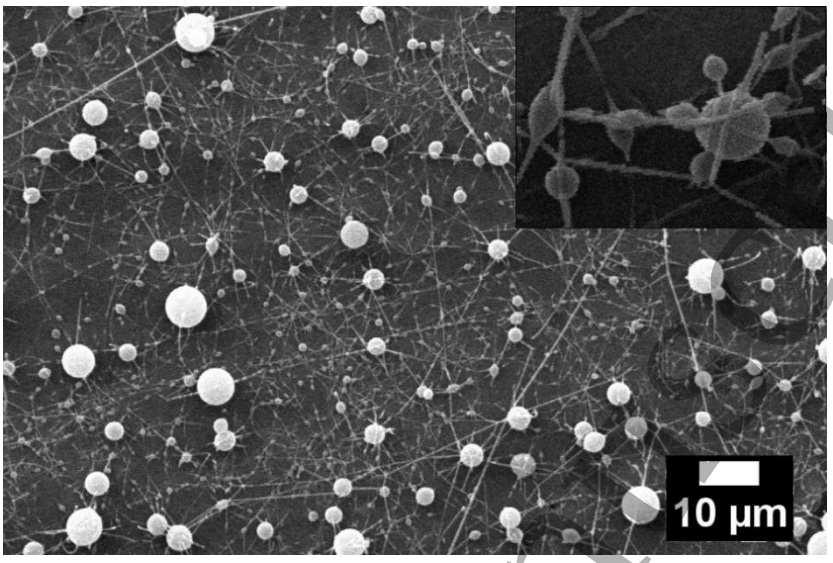

Figure 5. A typical SEM image of the electrospun PAN/Au sample from the dispersion of gold nanoparticles (0.01% w/v) in PAN solution (6 and 7 % w/v) under different electrospinning conditions

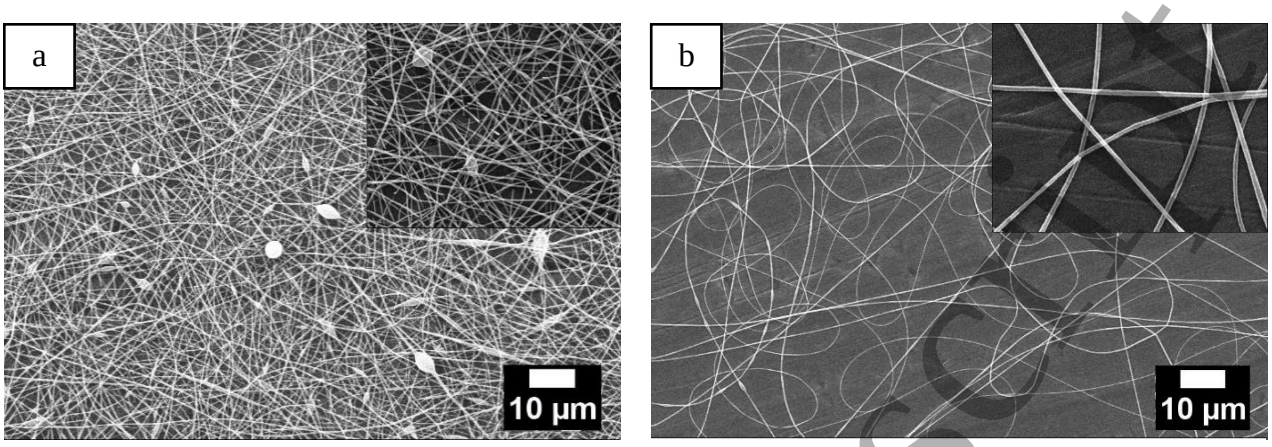

Figure 6. SEM images of the electrospun PAN/Au sample from the dispersion of gold nanoparticles (0.01% w/v) in different concentrations of PAN solution, (a) 8% w/v, (b) 9% w/v and, electrospinning conditions: voltage = 11 kV, nozzle – collector distance =15 cm, feed rate = 0.075 ml/h

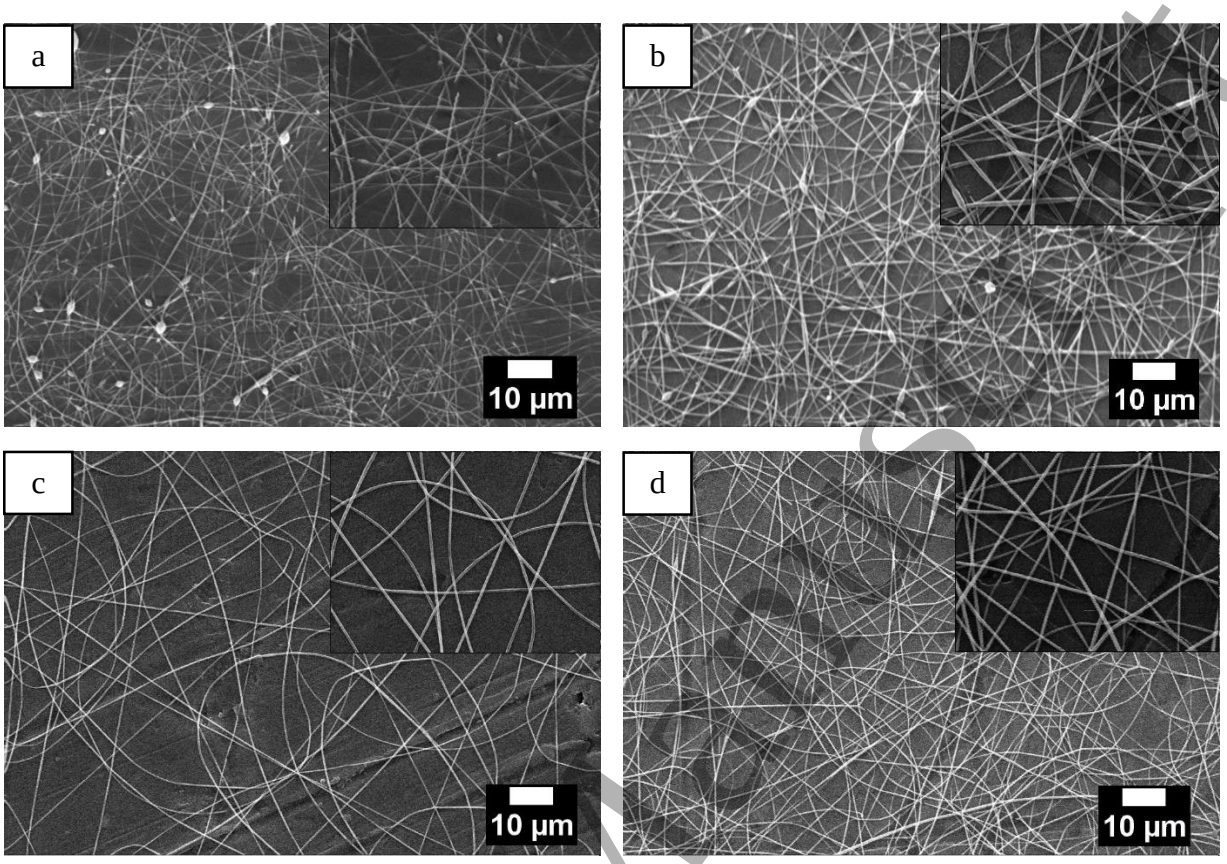

Figure 7. SEM images of the electrospun PAN/Au sample from the dispersion of gold nanoparticles (0.02% w/v) in different concentrations of PAN solution, (a) 6% w/v, (b) 7% w/v, (c) 8% w/v and (d) 9% w/v , electrospinning conditions: voltage = 11 kV, nozzle – collector distance =15 cm, feed rate = 0.075 ml/h

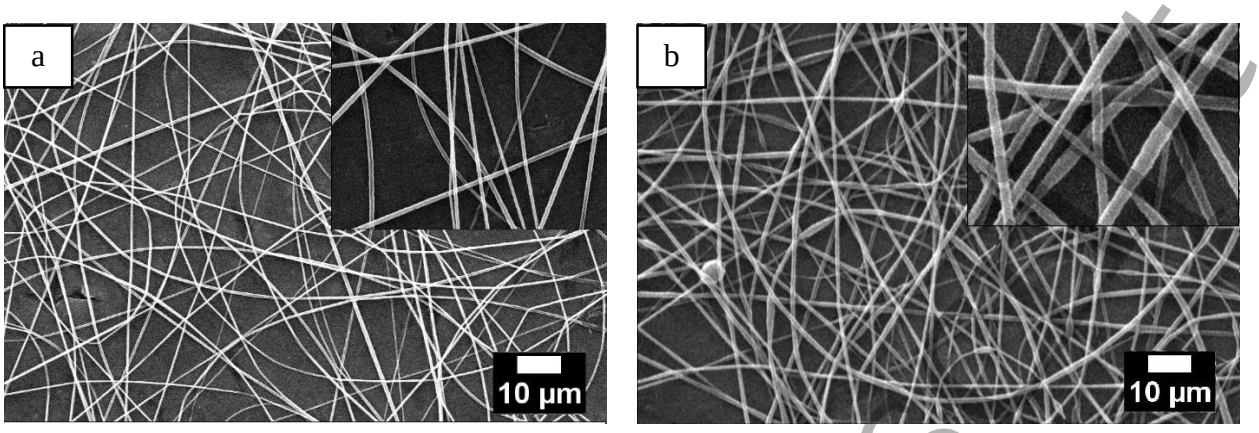

Figure 8. SEM images of the electrospun PAN/Au sample from the dispersion of gold nanoparticles (0.03% w/v) in different concentrations of PAN solution, (a) 6% w/v, (b) 7% w/v, electrospinning conditions: voltage = 11 kV, nozzle – collector distance =15 cm, feed rate = 0.075 ml/h

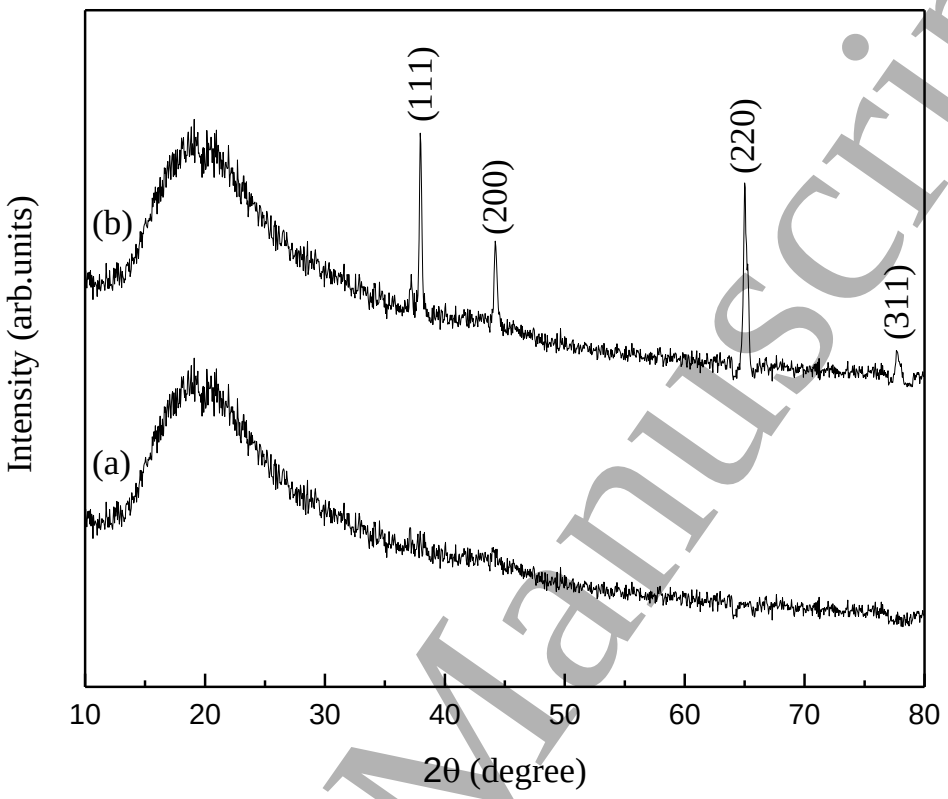

Figure 9. XRD patterns of electrospun (a) PAN nanofibers 12% w/v, (b) PAN/Au nanofibers from the dispersion of gold nanoparticles (0.02% w/v) in PAN solution 8% w/v, electrospinning conditions: voltage = 11 kV, nozzle – collector distance =15 cm, feed rate = 0.075 ml/h

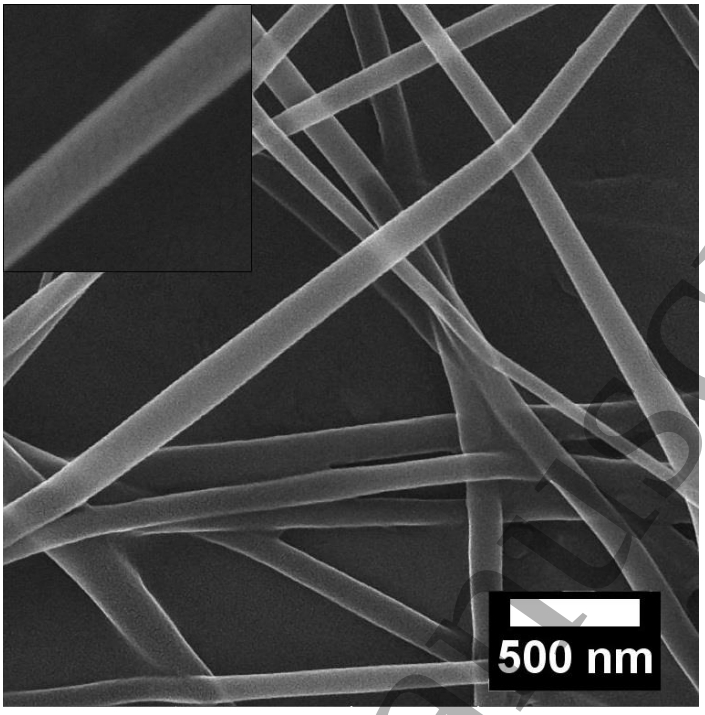

Figure 10. FESEM image of the electrospun PAN/Au sample from the dispersion of gold nanoparticles (0.02% w/v) in PAN solution 8% w/v, electrospinning conditions: voltage = 11 kV, nozzle – collector distance =15 cm, feed rate = 0.075 ml/h

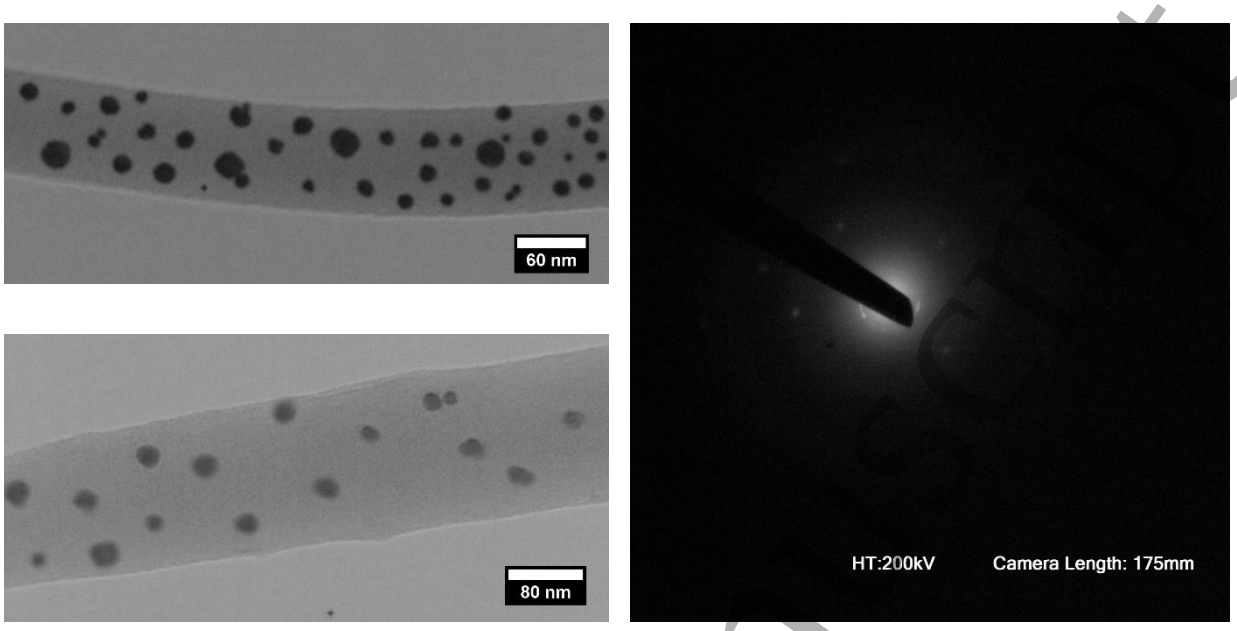

Figure 11. TEM images of the electrospun PAN/Au nanofibers from the dispersion of gold nanoparticles (0.02% w/v) in PAN solution 8% w/v, electrospinning conditions: voltage = 11 kV, nozzle – collector distance =15 cm, feed rate = 0.075 ml/h

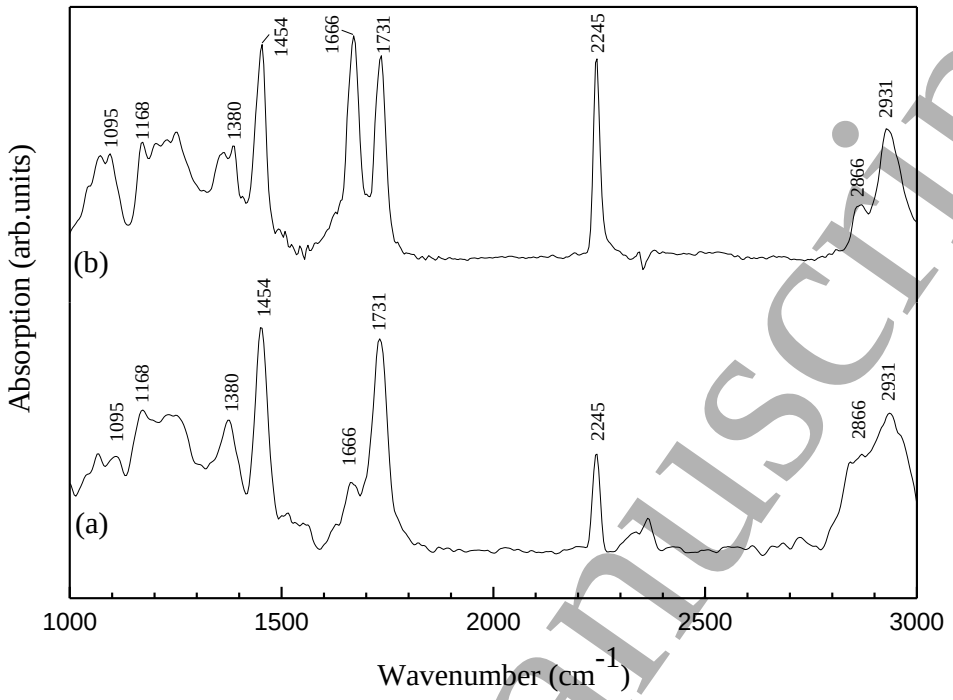

Figure 12. FTIR spectra of electrospun (a) PAN nanofibers 12% w/v, (b) PAN/Au nanofibers from the dispersion of gold nanoparticles (0.02% w/v) in PAN solution 8% w/v, electrospinning conditions: voltage = 11 kV, nozzle – collector distance =15 cm, feed rate = 0.075 ml/h

Table 1. Average diameter of the electrospun PAN/Au nanofibers (replica = 100) and the corresponding viscosity, electrical conductivity and surface tension of PAN/Au electrospinning solutions (replica = 5)

Average diameter of nanofibers (nm)	PAN concentration (% w/v)	Au nanoparticles concentration (% w/v)	Viscosity (cP)	Electrical conductivity (µs)	Surface tension ($mN.m^{-1}$)
-	6	0.01	75 (6.5)	119 (2)	38.04 (0.03)
-	7	0.01	115 (4)	115.6 (3.5)	37.49 (0.03)
317 (35)	8	0.01	166 (7)	111.2 (5)	36.64 (0.03)
-	9	0.01	270 (5)	107.1 (2.5)	36.78 (0.03)
-	6	0.02	117 (7)	156.7 (2.5)	37.77 (0.03)
-	7	0.02	154 (4.5)	151.4 (4)	36.94 (0.03)
123 (26)	8	0.02	223 (5)	149.3 (3.5)	36.29 (0.03)
176 (35)	9	0.02	318 (6)	142.3 (2)	36.56 (0.03)
140 (23)	6	0.03	264 (6)	212.6 (5.5)	37.54 (0.03)
244 (36)	7	0.03	349 (4)	204/5 (3)	37.03 (0.03)

(The numbers in the brackets show the standard deviation)